Technical requirements for practical implementation of fault passage indication

Technical requirements for practical implementation of fault passage indication

Amir Farughian
School of Technology and Innovations
University of Vaasa
Vaasa, Finland
amir.farughian@uva.fi

Lauri Kumpulainen
School of Technology and Innovations
University of Vaasa
Vaasa, Finland
lauri.kumpulainen@uva.fi

Kimmo Kauhaniemi
School of Technology and Innovations
University of Vaasa
Vaasa, Finland
kimmo.kauhaniemi@uva.fi

Seppo Pettissalo
Vaspec Oy
Vaasa, Finland
seppo.pettissalo@vaspec.fi

Ville Sallinen
Emtele Oy
Tampere, Finland
ville.sallinen@emtele.com

***Abstract*—One of the distinctive features of smart grids is feeder automation. Fault location is an important part of this feature and has become an essential function for distribution system operators. Reliable fault location expedites the restoration of power following an outage caused by a permanent fault. The most common type of faults in distribution networks is the single phase to ground fault. To locate earth faults in non-effectively earthed medium-voltage distribution networks, a number of methods have been put forward among which methods that are based on fault passage indication appear to be promising. This paper discusses the technical apparatus required for implementing two FPI-based methods in practice.**

Keywords— earth fault location, technical requirements, apparatus, application considerations, symmetrical sequence components

I. INTRODUCTION

Fault location has become an essential function for distribution system operators. Some permanent faults could lead to power outage. A reliable fault location method can help system operators to locate the actual fault in the network as soon as possible. The most common type of faults in distribution networks is the earth fault. Generally, faulty feeder identification and fault location in distribution networks could be performed at three levels:

1. Faulty feeder identification: Only the faulted feeder is determined. This is usually an integral part of the feeder relay protection.
2. Fault Passage Indication (FPI): The faulted section, e.g., lines or cables connecting two consecutive secondary substations on a radial feeder, is identified.
3. Distance estimation: The fault distance from the measurement point (usually the beginning of the faulted feeder) is estimated.

A number of methods have been proposed to locate earth faults in distribution networks [1].

- Impedance based methods [2] [3] [4]
- Injection methods [5]
- Voltage sag measured at the low voltage side of transformers at secondary substations [6]
- Traveling wave based methods [7]
- Signal processing [8] [9]
- Fault passage indicators (FPIs) [10] [11] [12] [13]

A comprehensive review on the state-of-the-art earth fault location methods along with their limitations is presented in [14]. One of the findings of Ref. [14] is that FPI-based methods appear to be a promising approach for locating earth faults in distribution networks. The purpose FPI-based methods is to find, on the faulty feeder, the faulted section i.e. the faulted segment linking two consecutive secondary substations. FPI aims at indicating if any fault current has passed through the measurement point at which the FPI device is installed. By installing multiple FPI devices at various locations (typically secondary substations) throughout the network, the faulted section identification can be achieved and visualized for the system operator. In general, the more FPI devices installed throughout the network, the more accurate fault location can be achieved. Two FPI-based methods have been presented by the authors in [12] and [13] which utilize current measurements and no voltage measurement is required. They have shown promising preliminary results in successfully identifying the points located on or off the fault passage. The methods employ symmetrical components of the currents to determine whether the FPI device is located on the fault passage or off the fault passage. In this paper, technical aspects and apparatus regarding the implementation of these methods in practice are discussed.

In Section II, the operational principles of the methods are presented shortly. Simulation results are used to help outlining the methods. In Section III, implementing the methods in practice is discussed in depth. Some field tests results are presented in Section IV. Conclusions are drawn in Section V.

II. METHOD OVERVIEW

A. Principles of operation

The method presented in [12] employs zero and negative sequence currents computed from measured phase currents. The negative sequence current (NSC) phasor for phase "a", by definition, is obtained as follows.

$$\bar{I}_2^{(a)} = \frac{1}{3}\left(\bar{I}_a + a^2\bar{I}_b + a\bar{I}_c\right) \quad (1)$$

Where, $\bar{I}_a, \bar{I}_b$ and $\bar{I}_c$ denote the phasors of phase currents of phases a, b and c, respectively and the operator a is $1\angle 120^0$. The phasor of the zero sequence current is calculated using the following equation.

$$\bar{I}_0 = \frac{1}{3}\left(\bar{I}_a + \bar{I}_b + \bar{I}_c\right) \quad (2)$$

The method presented in [12] is based on a finding that on the fault passage, both zero and negative sequence currents are significant whereas on points off the fault passage, only the zero sequence (ZSC) current is significant and the negative sequence current is negligible. Using this finding, the faulted segment can be identified.

The method presented in [13], requires only ZSC to locate the faulted segment. However, this method is applicable only to isolated networks. This method is based on the finding that ZSC on the faulty feeder increases from the beginning of the feeder up to the fault point.

B. Fault location procedure in practice

FPI devices that are installed along distribution feeders constantly measure phase currents and record the measurement data within a moving window of one second. Once the summation of phase currents or alternatively the zero sequence current measured by a device exceeds a pre-set threshold, that device gets triggered and saves the recorded measurement window so that the first half of the window contains measurements in no fault condition (pre-trigger period) and the second half contains during the fault condition data (post-trigger period). The device then sends the recording through 3G, 4G or 5G to a control center where the raw data is processed. In the control center, the phasors of the sequence currents are computed using equations (1) and (2) for both pre and post-fault periods. The fault passage indication then can be realized using method 1 and method 2.

1) Method 1

Based on the comparison of the computed negative and sequence currents between pre and post-fault periods, it is determined whether the device in question is located on the fault passage or off the fault passage. The control center carries out this analysis for every device whose recording has arrived to the control center. The devices with no recordings in the control center are determined to be located off the fault passage. The devices' locations are known to the control center. The faulted segment is determined to be the segment between the last device on the fault passage and the first device off the fault passage. Finally, the faulted segment is visualized on the map for the operator.

2) Method 2

The control center collects all the recordings that have arrived at around the same time. The amplitude of the phasor of ZSC of each recording is divided by the amplitude of the phasor of the ZSC of the first device (the device that is installed at the beginning of the feeder). If the result of this division is greater than one, then that device is determined to be located on the fault passage. Otherwise, the device is off the fault passage. Similarly, if a device has no recording in the group of recordings, that device is determined to be located off the fault passage. The faulted segment is determined to be the segment between the last FPI device on the fault passage and the first device off the fault passage. Finally, the faulted segment is visualized on the map for the system operator.

When there is an earth fault on the feeder, the ZSC at devices that are located after the fault point could be so tiny that it does not exceed the pre-set threshold and, as a result, the device will not get triggered. This is however, not a concern when it comes to fault passage indication as missing a recording from a device is an indication that the device in question is located after the fault point i.e. off the fault passage. The concept of fault passage indication is illustrated in Fig. 1.

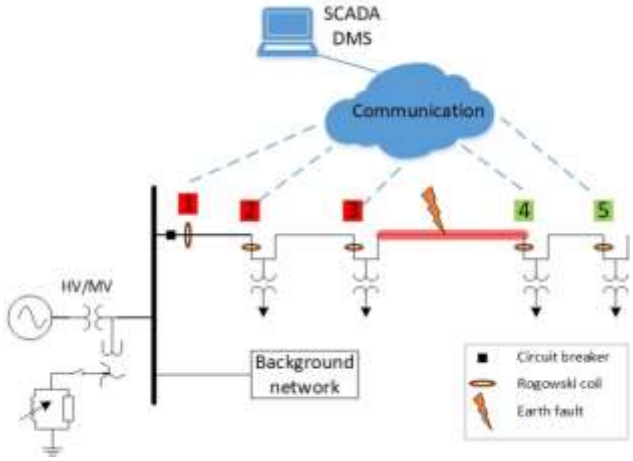

Fig. 1 Fault passage indication on a radial distribution feeder.

C. Simulation results

The operational principles of the methods can be better understood by way of example. The simulations are carried out using a verified model based on a real medium voltage distribution network in Finland. Fig. 2 shows the simplified diagram of the medium- voltage distribution network modeled in PSCAD™/EMTDC™. A 110 kV high-voltage network supplies the 20 kV medium-voltage network through a 40 MVA transformer. The network type from the viewpoint of neutral point treatment can alter between isolated and compensated. The medium-voltage network consists of several feeders from which a single one is depicted in the figure and the rest are shown as a single block "Background network". The fault occurs on the single feeder and therefore, the background network represents all the healthy feeders. The feeder under study consists of a mixture of underground cables and overhead lines. It has four secondary substations equipped with current measurements. Naturally, there is also a measurement point at the beginning of the feeder (at the primary substation). An earth fault occurs at one of the feeders on phase ''a'' between measurement points 3 and 4. The fault resistance is 0.01 Ω.

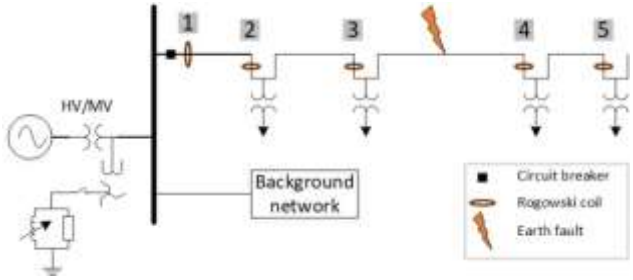

Fig. 2 Earth fault on a medium-voltage distribution network with four secondary substations equipped with Rogowski-coil-based current sensors.

Sequence currents at their steady state during the fault period can be calculated using equations (1) and (2). The calculated zero and negative sequence currents at the measurement points marked on Fig. 2 are shown in Fig. 3.

1) Compensated network

When the network is in its compensated mode i.e. the Petersen coil is connected to the neutral of the network, the NSC remains almost the same value of 3 A from measurement point 1 to measurement point 3. It is negligible at points 4 and 5. Therefore, one can identify the faulted segment using the NSC. The ZSC decreases from the beginning of the feeder towards the end.

2) Isolated network

When the network is in its isolated mode, it means the neutral point is disconnected from the Petersen coil. This results in higher fault current and consequently higher levels of zero and negative sequence currents. NSC remains almost at the same value of 32 A from measurement point 1 to measurement point 3 and is negligible after the fault point. The ZSC current increases slightly from point 1 towards point 3. After that, it drops. Therefore, one can determine the faulted segment using the ZSC alone.

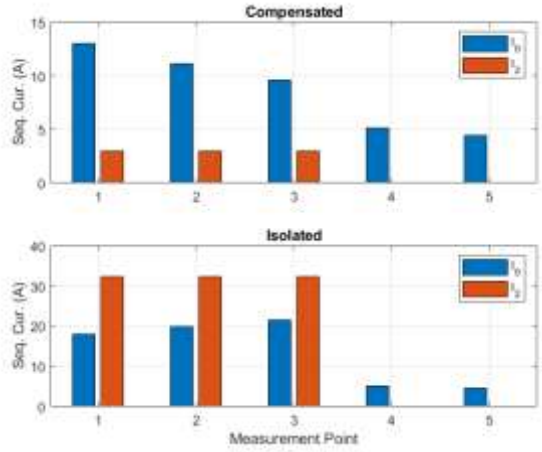

Fig. 3 Sequence currents during an earth fault obtained from the five measurement points shown in Fig. 2.

The calculated zero and negative sequence currents at various points on the faulted feeder are presented in Table 1 and Table 2 for two fault resistances of 0.01 Ω and 100 Ω. The values presented in the tables are calculated during the fault period. Under no fault condition, in a symmetrical network like the simulated model in question, negative and zero sequence currents are 0 A at any point along the distribution feeder. For this reason, the values presented in the tables are only from the during the fault period. Table 1 presents the sequence currents when the network is in its compensated mode.

Table 1. Zero and negative sequence currents at five measurement points for the network of Fig. 2 in its compensated mode.

	$R = 0.01\,\Omega$		$R = 100\,\Omega$		
MP	$I_0\,(A)$	$I_2\,(A)$	$I_0\,(A)$	$I_2\,(A)$	**FPI**
1	13.0	3.0	12.3	2.7	On
2	1.1	3.0	10.6	2.7	On
3	9.6	3.0	9.1	2.7	On
4	5.1	0	4.9	0	Off
5	4.4	0	4.3	0	Off

In Table 2, zero sequence currents for each measurement point are given. In addition, these values are scaled so that they are divided by the one from measurement point 1 (I_{0s}). According to method 2, if the scaled value is greater than or equal to 1, the measurement point in question is on the fault passage. Otherwise, it is off the fault passage.

Table 2. Zero sequence currents and their normalized values for the network of Fig. 2 in its isolated mode.

	$R = 0.01\,\Omega$		$R = 100\,\Omega$		
MP	$I_0\,(A)$	$I_0\,/I_{0s}$	$I_0\,(A)$	$I_0\,/I_{0s}$	**FPI**
1	18.0	1	15.8	1	On
2	19.9	2.5	17.5	1.1	On
3	21.5	2.7	18.9	1.2	On
4	5.1	0.6	4.5	0.3	Off
5	4.5	0.6	3.9	0.2	Off

III. Practical Aspects

A. Measurements

The proposed FPI methods require no voltage measurement. For measuring the phase currents required for implementing the FPI method, Rogowski-coil-based sensors are recommended. They have the advantage of being suitable for retrofit installations. In addition, unlike CTs, they do not saturate. A Rogowski coil current sensor is an air-core coil that warps around the cable or overhead line. The voltage signal induced in the coil is proportional to the derivative of the current flowing through the coil. Therefore, using an integration circuit or alternatively integrating on the software side, the voltage signal can be converted into a current signal. Since there is no iron core in the coil, no saturation takes place. As a result, current sensors are more accurate compared to conventional CTs. In addition, the coil's output is linear when subjected to large currents. This makes Rogowski-coil-based sensors suitable for measuring large fault currents in transmission and distribution networks. One other advantage that this type of sensor offers is that thanks to its low voltage output, it causes no hazard to personnel and equipment. In the practical implementation described below, the smallest measurable current level is 0.1 A. The Rogowski coils used in the implementation of the discussed methods have the accuracy of 0,5 %. The angle accuracy is about one degree.

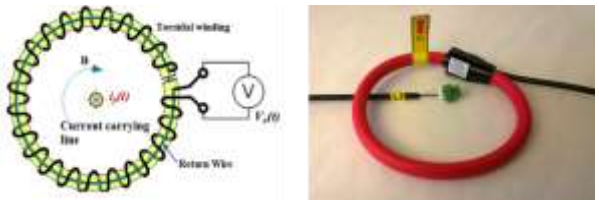

Fig. 4 Rogowski-coil-based current sensor [15].

To calculate the phasor of the NSC using equation (1), the phase angle of each phase current phasor is required. If one Rogowski is incorrectly installed in terms of polarity, it affects the phasor calculations. Therefore, it is essential that Rogowski coils for all phases are installed uniformly. Correct installation of Rogowski coils are shown in Fig. 5. The arrow marked on the sensor signifies the polarity.

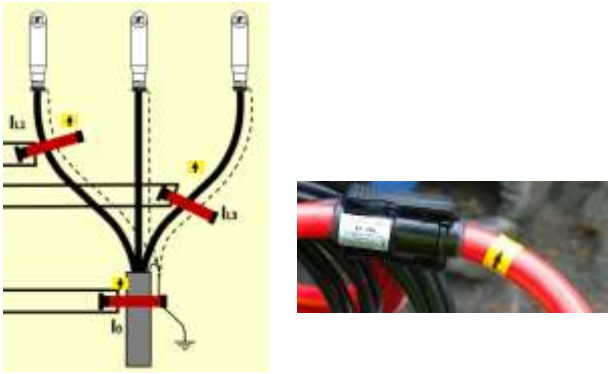

Fig. 5 Rogowski coil installation on a measurement point, arrrows show polarity.

B. Communication

In Fig. 6, the block diagram of an FPI unit connected to a remote secondary substation is illustrated. Some technical specifications of an FPI device are presented in Appendix. The recorded measurement along with the time stamp of the disturbance are sent to a control center. A modem embedded in the FPI device sends the recorded data to the control center. This is illustrated in Fig. 7.

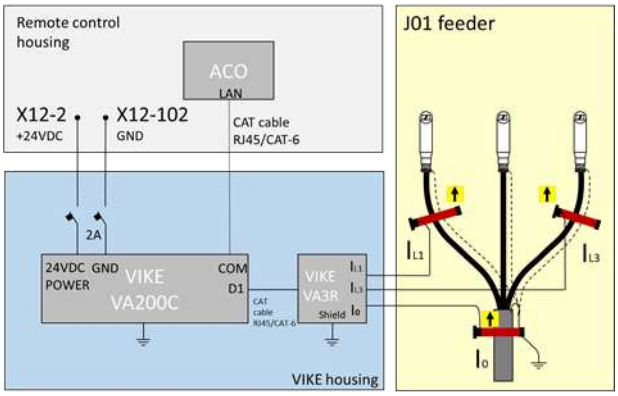

Fig. 6 Single FPI unit and its connection to a remote secondary substation.

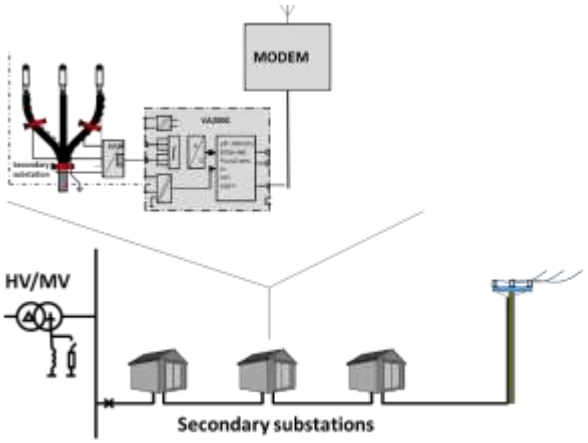

Fig. 7 Intelligent fault indicator at a secondary substation.

3G, 4G or 5G communication technology can be used for transferring the data. An alternative for sending the data to the control center is through the available automation systems at secondary substations using telecommunication protocol IEC 60870-5-104.

C. Data acquisition

1) Sampling rates

In the real world implementation, FPI devices constantly measure phase currents using two sampling rates of 1.6 and 25.6 kHz. The sampling rate of 1.6 kHz is used for detecting permanent earth faults and the sampling rate of 25.6 kHz is used to detect intermittent earth faults. An intermittent earth fault is a special type of fault, which is common mostly in compensated cable networks. It causes short current spikes whose durations are typically only 0.1 to 1 ms. If only the sampling rate of 1.6 kHz is used to measure currents, these spikes might be missed. Therefore, another set of measurements is carried out using the sampling rate of 25.6 kHz.

The length of the recording windows for both sets of measurements is the same in terms of samples, i.e. the number of samples for each phase current for each sampling rate is 1600. This means that the recording window of measurements obtained by sampling rate of 1.6 kHz is 1 s and the recording window of measurements obtained by sampling rate of 25.6 kHz is 0.0625 s.

2) Recording structure

An FPI device is triggered once the summation of phase currents (or alternatively the ZSC) that the device measures exceeds a pre-set threshold. The two sets of recordings that are obtained with two sampling rates are saved in the memory of the device. The modem embedded in the device sends the recording to the control center where the recordings are further analyzed. Each recording that arrives to the control center consists of two parts:

- pre-fault period
- during fault period

In an ideal network with no asymmetry, no ZSC or NSC exists in the network under normal condition. In practice, however, there could be cases where some level of NSC exists even when there is no actual earth fault. This could be, for example, due to unbalanced loads. In practice, one advantage that recording and analyzing the measurements in the pre-fault period provides is that there is no need to know the negative sequence current level of the network in no fault condition.

D. Sensitivity and network types

As mentioned before, the FPI device triggering mechanism is based on detecting an increase in the ZSC (or alternatively the summation of phase currents). The system operators can set the threshold of this increase remotely. In fact, the system operator can update the firmware of the device anytime remotely to achieve the desired sensitivity. For higher sensitivity, the system operator can configure the pre-set threshold to a lower value. The downside of the high sensitivity would be that many disturbances that are not actual earth faults could trigger devices. This leads to many recordings being unnecessarily sent to the control center for further processing.

In terms of the neutral point treatment, the discussed FPI methods are applicable to non-effectively grounded networks i.e.

- isolated neutral network
- centrally compensated network
- centrally and decentrally compensated network

The compensated network seems to be the most challenging type of network when it comes to earth fault location, as the fault current in this type of network could be very low. This is due to the fact that the Petersen coil (compensation coil) compensates the capacitive component of the fault current.

IV. FIELD TESTS

To examine the validity of the discussed methods, a series of disturbance recordings was performed on an MV distribution network in Finland (Fig. 8). The tests were carried out by DSOs in cooperation with network automation system providers in Finland. Current and voltage measurement devices were installed at the beginning of two feeders. The earth faults were applied to one of the feeders while the other feeder remained healthy. A set of raw recordings obtained from these two feeders during an earth fault test is presented in this section. Phase voltages measured at the primary substation are shown in Fig. 9. The faulted phase is "c", as can be seen. Phase currents of faulty and healthy feeders are shown in Fig. 10. For better readability, the figures have different scales.

Fig. 8 Field testing, courtesy of Maviko Oy.

The corresponding negative and zero sequence currents for the faulty and healthy feeders calculated using equations (1) and (2) are shown in Fig. 11. ZSC is significant in both feeders whereas NSC is negligible on the healthy feeder.

A. No fault period

For the healthy feeder, the no fault period is the period prior to $t = 2.5\ s$ and for the faulty feeder, the no fault period is the period prior to $t = 2.08\ s$. The zero sequence currents for faulty and healthy feeders are 0.65 and 0.35, respectively. The negative sequence currents are 0.10 and 0.45 A, respectively.

B. During fault period

For the faulty and faulty feeders, the during fault periods are the period after $t = 2.50\ s$ and $t = 2.08\ s$, respectively. The zero sequence currents for faulty and healthy feeders at their steady states are and zero sequence currents are 25.80 A and 15.10 A, respectively. The negative sequence currents at their steady states 5.60 A and 0.40 A.

Therefore, by comparing the sequence currents calculated for the two periods (before and during fault period), it can be readily determined if the measurement point in question is on or off the fault passage.

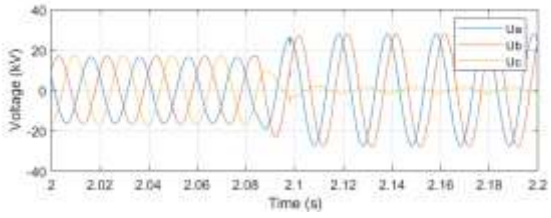

Fig. 9 Phase to ground voltages measured at the primary substation, faulted phase c, courtesy of Emtele Oy.

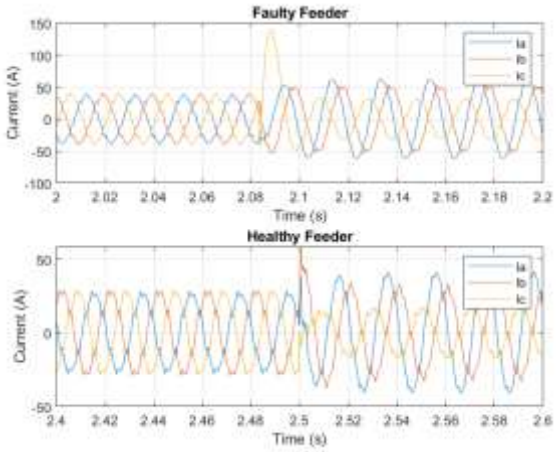

Fig. 10 phase currents measured at (the beginning of) faulty and healthy feeders, pre- and during fault periods, courtesy of Emtele Oy.

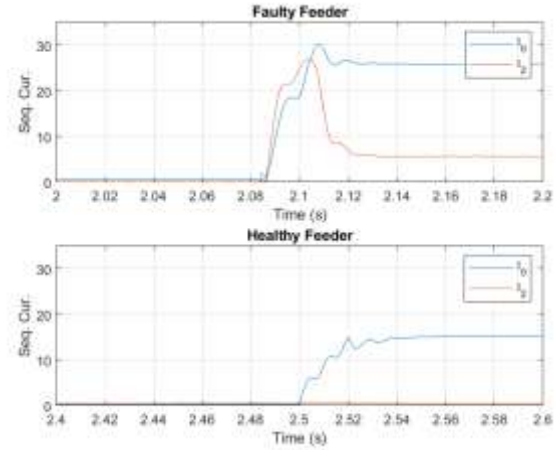

Fig. 11 sequence current calculated for the phase currents shown in Fig. 10.

V. CONCLUSION

The technical apparatus required for implementing two FPI-based methods in practice was discussed in depth. It appears the presented methods can be successfully implemented in practice. However, the methods are applicable to high-impedance earth faults as long as the resulting fault current causes large enough sequence currents that are measureable. The FPI-based methods required no voltage measurement. In addition, the operational principles of the methods were outlined with the help of simulations. Technical aspects such as fault location procedure, measurement, sensitivity of the method, the required communication, network types, etc. were covered in the discussion.

VI. APPENDIX

Operating voltage	8… 36 VDC
Current measurement	2x3 / Rogowski coils
Digital outputs	2
Communication	Ethernet
Protocol	IEC 60870-5-104
Software can be updated remotely	
Phase current measurement	0…2500 A
Residual current measurement	0…250 A
Serial buses	1 for the expansion unit
A / D converter	16 bit
Sampling frequency	25.6 kHz / channel
Fault recorder	For transients and RMS values of currents

Phase voltage measurement (option)	capacitive or resistive
Housing	DIN rail mounted

REFERENCES

[1] "IEEE Guide for Determining Fault Location on AC Transmission and Distribution Lines," *IEEE Std C37.114-2014 (Revision of IEEE Std C37.114-2004)*, pp. 1–76, Jan. 2015, doi: 10.1109/IEEESTD.2015.7024095.

[2] "Comparison of Impedance Based Location Methods for Power Distribution Systems," *Elsevier, Electric Power Systems Research,* vol. 78, no. 4, pp. 657–666, 2008.

[3] A. Nikander and P. Järventausta, "Identification of High-Impedance Earth Faults in Neutral Isolated or Compensated MV Networks," *IEEE Transactions on Power Delivery*, vol. 32, no. 3, pp. 1187–1195, Jun. 2017, doi: 10.1109/TPWRD.2014.2346831.

[4] J. Altonen and A. Wahlroos, "Advancements in fundamental frequency impedance based earth fault location in unearthed distribution systems," presented at the CIRED 19th International Conference on Electricity Distribution, Vienna, May 2007, [Online]. Available: https://pdfs.semanticscholar.org/37cc/a4bb8b1037b6ba840014b869f6b491bdcbb7.pdf.

[5] G. Druml, C. Raunig, P. Schegner, and L. Fickert, "Fast selective earth fault localization using the new fast pulse detection method," in *22nd International Conference and Exhibition on Electricity Distribution (CIRED 2013)*, Jun. 2013, pp. 1–5, doi: 10.1049/cp.2013.1068.

[6] D. Topolanek, M. Lehtonen, M. R. Adzman, and P. Toman, "Earth fault location based on evaluation of voltage sag at secondary side of medium voltage/low voltage transformers," *IET Generation, Transmission & Distribution*, vol. 9, no. 14, pp. 2069–2077, 2015, doi: 10.1049/iet-gtd.2014.0460.

[7] G. Druml, O. Skrbinjek, W. Hipp, L. Fickert, U. Schmidt, and P. Schegner, "First results concerning localisation of earthfaults in compensated 20-kV-networks based on travelling waves," presented at the 25th International Conference on Electricity Distribution (CIRED 2019), Madrid, Jun. 2019, Accessed: Jan. 23, 2020. [Online]. Available: https://www.cired-repository.org/handle/20.500.12455/160.

[8] N. I. Elkalashy, M. Lehtonen, H. A. Darwish, A.-M. I. Taalab, and M. A. Izzularab, "Operation evaluation of DWT-based earth fault detection in unearthed MV networks," in *2008 12th International Middle-East Power System Conference*, Mar. 2008, pp. 208–212, doi: 10.1109/MEPCON.2008.4562385.

[9] N. I. Elkalashy, N. G. Tarhuni, and M. Lehtonen, "Simplified probabilistic selectivity technique for earth fault detection in unearthed MV networks," *Transmission Distribution IET Generation*, vol. 3, no. 2, pp. 145–153, Feb. 2009, doi: 10.1049/iet-gtd:20070523.

[10] J. Altonen and A. Wahlroos, "Performance of modern fault passage indicator concept in compensated MV-networks," in *CIRED Workshop 2016*, Jun. 2016, pp. 1–4, doi: 10.1049/cp.2016.0733.

[11] J. Altonen, A. Wahlroos, S. Vähäkuopus, and E. Oy, "Application of multi-frequency admittance-based fault passage indication in practical compensated MV-network," Glasgow, Jun. 2017, p. 5.

[12] Farughian, Kumpulainen, and Kauhaniemi, "Earth Fault Location Using Negative Sequence Currents," *Energies*, vol. 12, no. 19, p. 3759, Sep. 2019, doi: 10.3390/en12193759.

[13] A. Farughian, L. Kumpulainen, and K. Kauhaniemi, "Non-Directional Earth Fault Passage Indication in Isolated Neutral Distribution Networks," *Energies*, vol. 13, no. 18, p. 4732, Jan. 2020, doi: 10.3390/en13184732.

[14] A. Farughian, L. Kumpulainen, and K. Kauhaniemi, "Review of methodologies for earth fault indication and location in compensated and unearthed MV distribution networks," *Electric Power Systems Research*, vol. 154, pp. 373–380, Jan. 2018, doi: 10.1016/j.epsr.2017.09.006.

[15] L. Kumpulainen, G. A. Hussain, M. Lehtonen, and J. A. Kay, "Preemptive Arc Fault Detection Techniques in Switchgear and Controlgear," *IEEE Transactions on Industry Applications*, vol. 49, no. 4, pp. 1911–1919, Jul. 2013, doi: 10.1109/TIA.2013.2258314.